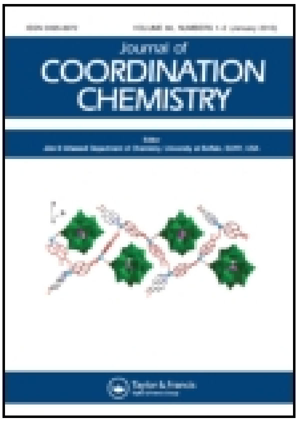

Journal of Coordination Chemistry
Publication details, including instructions for authors and subscription information:
http://www.tandfonline.com/loi/gcoo20

Sandwich-type polyoxometalates of the later lanthanide ions. Syntheses and structures of $[(A\text{-}XW_9O_{34})_2(H_2OM)_3CO_3]^{11-}$ ($X=P^{5+}$, As^{5+}) ($M=Tb^{3+}$, Dy^{3+}, Er^{3+})

Roushan Khoshnavazi [a] , Francesco Nicolò [b] , Hadi Amiri Rudbari [c] , Elham Naseri [a] & Ahmad Aminipour [a]

[a] Department of Chemistry , University of Kurdistan , Sanandaj , Iran

[b] Dipartimento di Chimica Inorganica, Chimica Analitica e Chimica Fisica , Università di Messina , Messina , Italy

[c] Faculty of Chemistry , University of Isfahan , Isfahan , Iran

To cite this article: Roushan Khoshnavazi , Francesco Nicolò , Hadi Amiri Rudbari , Elham Naseri & Ahmad Aminipour (2013) Sandwich-type polyoxometalates of the later lanthanide ions. Syntheses and structures of $[(A\text{-}XW_9O_{34})_2(H_2OM)_3CO_3]^{11-}$ ($X=P^{5+}$, As^{5+}) ($M=Tb^{3+}$, Dy^{3+}, Er^{3+}), Journal of Coordination Chemistry, 66:8, 1374-1383, DOI: 10.1080/00958972.2013.782006

To link to this article: http://dx.doi.org/10.1080/00958972.2013.782006

Journal of Coordination Chemistry, 2013
Vol. 66, No. 8, 1374–1383, http://dx.doi.org/10.1080/00958972.2013.782006

Taylor & Francis
Taylor & Francis Group

Sandwich-type polyoxometalates of the later lanthanide ions. Syntheses and structures of $[(\text{A-XW}_9\text{O}_{34})_2(\text{H}_2\text{OM})_3\text{CO}_3]^{11-}$ $(\text{X} = \text{P}^{5+}, \text{As}^{5+})$ $(\text{M} = \text{Tb}^{3+}, \text{Dy}^{3+}, \text{Er}^{3+})$

ROUSHAN KHOSHNAVAZI*†, FRANCESCO NICOLÒ‡, HADI AMIRI RUDBARI§,
ELHAM NASERI† and AHMAD AMINIPOUR†

†Department of Chemistry, University of Kurdistan, Sanandaj, Iran
‡Dipartimento di Chimica Inorganica, Chimica Analitica e Chimica Fisica, Università di Messina, Messina, Italy
§Faculty of Chemistry, University of Isfahan, Isfahan, Iran

(*Received 16 May 2012; in final form 4 January 2013*)

Six new complexes were synthesized in a 0.1 M aqueous carbonate solution and characterized by elemental analyses, thermogravimetric analyses, infrared spectroscopy and X-ray single crystal structure analyses. The single-crystal structure analysis was on $K_{11}[(A\text{-}AsW_9O_{34})_2(H_2ODy)_3CO_3]\cdot 22H_2O$. The results revealed that the complexes are isomorphic and their structures consist of two lacunary $[A\text{-}XW_9O_{34}]^{9-}$ Keggin moieties linked by a $(OMOH_2)_3C$ belt, forming an A-type sandwich structure. The CO_3^{2+} is tridentate and fixes three M^{3+} centers together by its oxygens. Each M^{3+} cation is mono-capped trigonal-prismatic coordination, achieved by two terminal oxygens of an edge-shared pair of WO_6 octahedra to each $[A\text{-}XW_9O_{34}]^{9-}$ and two oxygens from the belt, and the cap by one water.

Keywords: Polyoxometalate; Sandwich-type complex; Later lanthanide ions; Tridentate carbonate ligand; Single crystal structure analysis

1. Introduction

Polyoxometalates (POMs), as versatile metal-oxygen cluster complexes, attract interest due to their topological properties and their potential applications in catalysis, photoluminescence, electrochromism and magnetism [1–8]. The lacunary POMs, as an important class of polyoxometalates, are derived from Keggin and Dawson structure by removing one, two, or three WO_6 octahedra units. A large number of these complexes incorporate pairs of trivacant lacunary anions that sandwich three or four metal atoms [9–16]. Attention has focused on developing polyoxometalate-based lanthanide complexes by incorporating Ln ions into lacunary POMs; such lanthanide–polyoxometalate derivatives have structural variety and interesting properties in fields including catalysis, magnetism, luminescence and materials science [17–25]. The first complex of Keggin trilacunary derivative with lanthanide ions, $[(PW_9O_{34})_2Ce_3O_3(OH_2)_2]^{12-}$,

---

*Corresponding author. Emails: r.khoshnavazi@uok.ac.ir; khoshnavazi@yahoo.com

was reported by Knoth [26]. In 2003, lanthanide complexes of $[(PW_9O_{34})_2Ln_3O_3(OH_2)_2]^{15-}$ (Ln = Ce^{3+}, La^{3+}) were reported [27]. These complexes have sandwich-type structures with two A-$[XW_9O_{34}]^{9-}$ units connected by a belt containing three oxygens, alternating with the three lanthanides. Hill synthesized the first examples of sandwich-type POMs that encapsulate CO_3^{2-} in the center of $[(A\text{-}PW_9O_{34})_2(H_2OY)_3CO_3]^{11-}$ [28]. We have synthesized the first lanthanide derivatives of this category $[(A\text{-}PW_9O_{34})_2(H_2OM)_3CO_3]^{11-}$ (M = Eu^{3+}, Gd^{3+}) formed by the reaction of A-α-$[PW_9O_{34}]^{9-}$ with M^{3+} in an aqueous Na_2CO_3 solution in modest yield and in high purity [29]. Divalent metal derivatives of the A-type sandwich complexes are unstable, converting to complexes containing B-$[XW_9O_{34}]^{n-}$ [30–32]. However, the title complexes with trivalent lanthanides are stable toward A to B isomerization and also allow stabilization of the encapsulated carbonate.

The title sandwich-type complexes have been isolated and characterized by elemental analysis, thermogravimetric analysis (TGA), FT-IR spectroscopy, magnetic properties, and single-crystal structure analysis.

2. Experimental

2.1. *Chemicals and apparatus*

All reagents were commercially obtained and used without purification. $ErCl_3\cdot 6H_2O$, $DyCl_3\cdot 6H_2O$ and $TbCl_3\cdot 6H_2O$ were purchased from Alfa Aesar Company. $Na_8H[A\text{-}PW_9O_{34}]\cdot xH_2O$ and $Na_8H[A\text{-}AsW_9O_{34}]\cdot xH_2O$ were prepared according to the literature [14, 33]. FT-IR spectra were recorded in KBr plates on a Bruker model Vector-22 Spectrophotometer. Electronic spectra were recorded on a UV–Vis spectrophotometer model Cary-Varian100. TGA was carried out using a PL-1500 TGA apparatus. ICP was used for the elemental analysis of terbium, dysprosium, erbium, and tungsten and flame photometry was used for analysis of sodium and potassium. TGA was used for the analysis of carbon and the crystallization water. Magnetic susceptibility data χ_g were obtained by using a Sherwood Scientific MSB-Auto magnetic susceptibility balance at room temperature (300 K). Strongly acidic (Dowex HCR-W_2 H^+ form) and basic (Amberjet 4200 Cl^- form) resins were packed into a column (20 cm length; 1 cm diameter) and were used for ion-exchange chromatography. For acidification, solutions of the complexes were eluted through the acidic form of the cationic resin column. For cation exchange, first 1 M L^{-1} KOH was eluted through the acidic form of the cationic resin followed by distilled water and then solutions of the complexes. The eluants were collected and studied by IR spectroscopy after solvent evaporation.

2.2. *Preparation of complexes*

2.2.1. $K_9Na_2[(A\text{-}PW_9O_{34})_2(H_2OTb)_3CO_3]\cdot 20H_2O$ (1). $TbCl_3\cdot 6H_2O$ (0.59 g, 1.6 mM) was dissolved in 20 mL of distilled water and 2 mL of 1 M L^{-1} Na_2CO_3 was slowly added to the solution with stirring. The slurry was heated to 80 °C and then solid $Na_8H[A\text{-}PW_9O_{34}]\cdot xH_2O$ (2.03 g, 0.8 mM) was quickly added with vigorous stirring. The solution was maintained at 80 °C for 30 min and then cooled to room temperature. Insoluble materials were removed by centrifugation. Solid KCl (2.0 g) was added and the solution was cooled in an ice water bath and then filtered. The crude product was recrystallized at least twice in hot water. Colorless crystals were obtained by slow evaporation. Yield: 0.85 g, 37.44%. Anal. Calcd for $K_9Na_2[(A\text{-}PW_9O_{34})_2(H_2OTb)_3CO_3]\cdot 20H_2O$ (%): C, 0.205; Na, 0.78; K, 6.02; W, 56.66; Tb, 8.16; and H_2O, 6.16. Found (%): C, 0.21; Na, 0.77; K, 6.0; W, 56.20; Tb, 8.06; and H_2O, 6.30.

2.2.2. $K_9Na_2[(A\text{-}PW_9O_{34})_2(H_2ODy)_3CO_3]\cdot 25H_2O$ (2). The procedure for **1** was repeated, but $DyCl_3\cdot 6H_2O$ (0.59 g) was used instead of $TbCl_3\cdot 6H_2O$. Yield: 0.88 g, 38.06%. Anal. Calcd for $K_9Na_2[(A\text{-}PW_9O_{34})_2(H_2ODy)_3CO_3]\cdot 25H_2O$ (%): C, 0.20; Na, 0.77; K, 5.92; W, 55.70; Dy, 8.20; and H_2O, 7.57. Found (%): C, 0.26; Na, 0.76; K, 5.86; W, 55.02; Dy, 7.67; and H_2O, 7.61.

2.2.3. $K_9Na_2[(A\text{-}PW_9O_{34})_2(H_2OEr)_3CO_3]\cdot 20H_2O$ (3). The procedure for **1** was repeated, but $ErCl_3\cdot 6H_2O$ (0.61 g) was used instead of $TbCl_3\cdot 6H_2O$. Yield: 0.97 g, 42.37%. Anal. Calcd for $K_9Na_2[(A\text{-}PW_9O_{34})_2(H_2OEr)_3CO_3]\cdot 20H_2O$ (%): C, 0.20; Na, 0.78; K, 6.0; W, 56.42; Er, 8.55; and H_2O, 6.13. Found (%): C, 0.20; Na, 0.77; K, 6.0; W, 55.62; Er, 7.67; and H_2O, 6.13.

2.2.4. $K_9Na_2[(A\text{-}AsW_9O_{34})_2(H_2OTb)_3CO_3]\cdot 22H_2O$ (4). The procedure for **1** was repeated, but $Na_8H[A\text{-}AsW_9O_{34}]\cdot xH_2O$ (2.03 g, 0.8 mM) was used instead of $Na_8H[A\text{-}PW_9O_{34}]\cdot xH_2O$. Yield: 0.74 g, 32.45%. Anal. Calcd for $K_9Na_2[(A\text{-}AsW_9O_{34})_2(H_2OTb)_3CO_3]\cdot 22H_2O$ (%): C, 0.20; Na, 0.77; K, 5.93; W, 55.78; Tb, 8.03; and H_2O, 6.67. Found (%): C, 0.20; Na, 0.79; K, 6.08; W, 54.79; Tb, 7.80; and H_2O, 6.63.

2.2.5. $K_{11}[(A\text{-}AsW_9O_{34})_2(H_2ODy)_3CO_3]\cdot 22H_2O$ (5). The procedure for **4** was repeated, but $DyCl_3\cdot 6H_2O$ (0.59 g) was used instead of $TbCl_3\cdot 6H_2O$. Yield: 0.76 g, 34.00%. Anal. Calcd for $K_{11}[(A\text{-}AsW_9O_{34})_2(H_2ODy)_3CO_3]\cdot 22H_2O$ (%): C, 0.20; K, 7.20; W, 55.38; Dy, 8.16; and H_2O, 6.62. Found (%): C, 0.20; K, 7.24; W, 54.02; Dy, 8.8; and H_2O, 6.58.

2.2.6. $K_{11}[(A\text{-}AsW_9O_{34})_2(H_2OEr)_3CO_3]\cdot 22H_2O$ (6). The procedure for **4** was repeated, but $ErCl_3\cdot 6H_2O$ (0.61 g) was used instead of $TbCl_3\cdot 6H_2O$. Yield: 0.87 g, 37.80%. Anal. Calcd for $K_{11}[(A\text{-}AsW_9O_{34})_2(H_2OEr)_3CO_3]\cdot 22H_2O$ (%): K, 7.18; W, 55.25; and Er, 8.37. Found (%): K, 7.00; W, 54.30; and Er, 8.23.

2.3. *X-ray crystallographic structure determination*

We attempted to obtain single crystal for all the six compounds but were only successful for **5**. Crystal data collection and refinement parameters for **5** are given in table 1. The data were collected at 296(2) K on a Bruker APEX2 CCD area detector single-crystal diffractometer with graphite monochromated Mo Kα radiation ($\lambda = 0.71073$ Å). Data collection, indexing, and initial cell refinements were all handled using APEX2 and SAINT (Bruker, 2005) software [34]. About 368,412 intensities were collected up to $2\theta = 53°$ and corrected by absorption using the semi-empirical method of equivalents. Structure was refined by weighted full-matrix least-squares on F^2 using 10,064 independent reflections. Due to the large disorder of solvation H_2O, water oxygens could not be located uniquely on the electron density maps and their hydrogens were omitted in the crystal model. The structure model shows the effects of this disorder mainly on large thermal ellipsoids of several water oxygens and on the final Fourier syntheses evidencing significant electron density residuals that could not be interpreted. Structure solution and refinement were all handled using

Table 1. Crystal data and structure refinement for **5**.

Empirical formula	$CH_{22}As_2Dy_3K_8Na_3O_{82}W_{18}$
Formula weight	5674.6
Temperature	296(2) K
Wavelength	0.71073 Å
Crystal system	Orthorhombic
Space group	Pnma
Unit cell dimensions	$a = 34.520(3)$ Å $b = 16.640(1)$ Å $c = 16.349(1)$ Å
Volume	9391(1) $Å^3$
Z	4
Calculated density	4.013 $Mg\,m^{-3}$
Absorption coefficient	25.465 mm^{-1}
$F(0\,0\,0)$	9860
Crystal size	0.30 × 0.25 × 0.15 mm
Theta range for data collection	1.72 to 26.50°
Limiting indices	$-43 \leqslant h \leqslant 43$, $-20 \leqslant k \leqslant 20$, $-20 \leqslant l \leqslant 20$
Reflections collected/unique	368,412/10,062 [$R_{(int)} = 0.0827$]
Completeness to theta = 26.50°	99.9%
Refinement method	Full-matrix least-squares on F^2
Data/restraints/parameters	10,062/0/589
Goodness-of-fit on F^2	1.239
Final R indices [$I > 2\sigma(I)$]	$R_1 = 0.0475$, $wR_2 = 0.1236$
R indices (all data)	$R_1 = 0.0600$, $wR_2 = 0.1465$
Largest difference in peak and hole	7.964 and −2.359 e A^{-3}

Table 2. The averaged bond lengths and corresponding bond valance values of **5**.

Bond	Bond length (Å)	Bond valance value
As–O	1.68(2)	1.27
W–O_d	1.72(2)	1.62
W–$O_{b,c}$	1.90(1)	1.04
W–O(As)	2.36(3)	0.34
W–O_d	1.79(3)	1.36
C–O	1.28(3)	1.35
Dy–O(H_2O)	2.34(6)	0.40
Dy–O(C)	2.45(3)	0.30
Dy–O_d	2.28(4)	0.47

SHELX-97 package [35]. Scattering factors and anomalous dispersion corrections were taken from the International Tables for X-ray Crystallography [36]. Selected bond parameters of **5** are given in table 2.

3. Results and discussion

3.1. *Syntheses and stabilities*

$[A\text{-}XW_9O_{34}]^{9-}$ ($X = P^{5+}$, As^{5+}) reacts with aqueous (0.1 M) Na_2CO_3 solution of MCl_3 ($M = Tb^{3+}$, Dy^{3+}, and Er^{3+}) to form **1–6** in modest yields. By adding sodium carbonate solution to the MCl_3 solution metal carbonate is formed, then $[A\text{-}XW_9O_{34}]^{9-}$ reacts with insoluble metal carbonate (the solution becomes clearer). Unlike $[(A\text{-}XW_9O_{34})_2(H_2OSm)_3\text{-}CO_3]^{11-}$ ($X = P^{5+}$, As^{5+}) [37], **1–3** are stable at high temperature. When solutions of the complexes were loaded onto the sodium form ($P\text{-}SO_3^-K^+$) of the cation-exchange column, no retention of the complexes was observed. The FT-IR spectrum of each individual eluant confirmed the integrity of the eluted parent complex. In a second series of experiments, solutions of the complexes were loaded onto an anion-exchange column in its Cl^- form, $P\text{-}NR_3^+Cl^-$. In this case, both anionic complexes were retained on the column. Control experiments were carried out with aqueous solutions of MCl_3; as expected the lanthanide cations were retained on the cation-exchange column but passed through the anion-exchange column. Consequently, these simple ion-exchange experiments provide good evidence for inner-sphere bonding of the lanthanide cations to $[XW_9O_{34}]^{9-}$ [27]. All of the complexes lose lanthanide ions upon passing through a strongly acidic ion-exchange column. Decomposition of the complexes takes place by dissolving them in 10^{-2} M HCl and NaOH. Experimental results show that the complexes are stable from pH 4 to 10. These observations are unlike the A-type sandwiches based on divalent d-block metals [15, 26].

3.2. *IR spectra*

Characteristic bands in all the complexes are 1470–1488 cm^{-1}, assigned to the doubly degenerate ν_3 of coordinated CO_3^{2-} with a small splitting of 10 cm^{-1} [38]. The ν_3 stretch frequencies increase with coordination of carbonate to lanthanide in comparison to free carbonate; thus, we conclude that $CO_3{}^{2-}$ coordinates more strongly in **1–6** than isostructure polyoxometalates of the earlier lanthanide ions of $[(A\text{-}\beta\text{-}GeW_9O_{34})_2(SmOH_2)_3CO_3]^{13-}$ [39] and $[(A\text{-}PW_9O_{34})_2(MOH_2)_3CO_3]^{11-}$ ($M = Eu^{3+}$, Gd^{3+}) [29]. Bond strength of coordinated carbonate with the lanthanide ions is a function of the lanthanide ion size. The smaller lanthanides make stronger bonds with oxygens of carbonate. The other two infrared active modes, ν_2 and ν_4, overlap with W–O stretching bands [28]. IR spectra of the sandwich type polyoxometalates $[(A\text{-}PW_9O_{34})_2(H_2OM)_3CO_3]^{11-}$ ($M = Tb^{3+}$, Dy^{3+}, and Er^{3+}) as well as $[(A\text{-}AsW_9O_{34})_2(H_2OM)_3CO_3]^{11-}$ ($M = Tb^{3+}$, Dy^{3+}, and Er^{3+}) are very similar (figure 1) and are also similar to that of $[A\text{-}XW_9O_{34}]^{9-}$. Comparing IR spectra of the complexes and trivacant lacunary $[A\text{-}XW_9O_{34}]^{9-}$, a shift of the stretch in the 700–1200 cm^{-1} range to higher frequencies is attributed to the decrease of negative charge per $[A\text{-}XW_9O_{34}]^{9-}$ in the anions. At 700–1000 cm^{-1}, bands were assigned to the asymmetric stretch of the $W\text{–}O_c\text{–}W$ (700–780 cm^{-1}) and $W\text{–}O_b\text{–}W$ (870–920 cm^{-1}) bridges and of the $W\text{–}O_d$ terminal bonds (940–947 cm^{-1}) (O_d is a terminal oxygen, O_b is a bridging oxygen between corner-sharing octahedra, and O_c is a bridging oxygen between edge-sharing octahedra). Bands at 1010 and 1060 cm^{-1} in **1**, **2,** and **3** were assigned to asymmetric stretching vibrations of (ν_3 vibrational mode) PO_4 with splitting due to the loss of local symmetry as expected for A-type trivacant Keggin unit, but that of AsO_4 for **4**, **5,** and **6** overlaps with the $W\text{–}O_b\text{–}W$ bond [29, 40].

3.3. *Thermogravimetric analysis*

The TGA was performed under N_2 from 28 to 600 °C. The thermal stability and decomposition characteristics of compounds in the solid state were assessed by TGA. Two distinct mass loss regions are observed below 520 °C [28, 37]. The first, 28–360 °C, is assigned to lattice and coordinated water (bonded to M^{3+}) loss and the second region, 460–600 °C for **1–3** and 418–600 °C for **4–6**, is assigned to loss of one molecule of CO_2 from the decomposition of CO_3^{2-}. The TGA curves show that phosphorus-based complexes lose

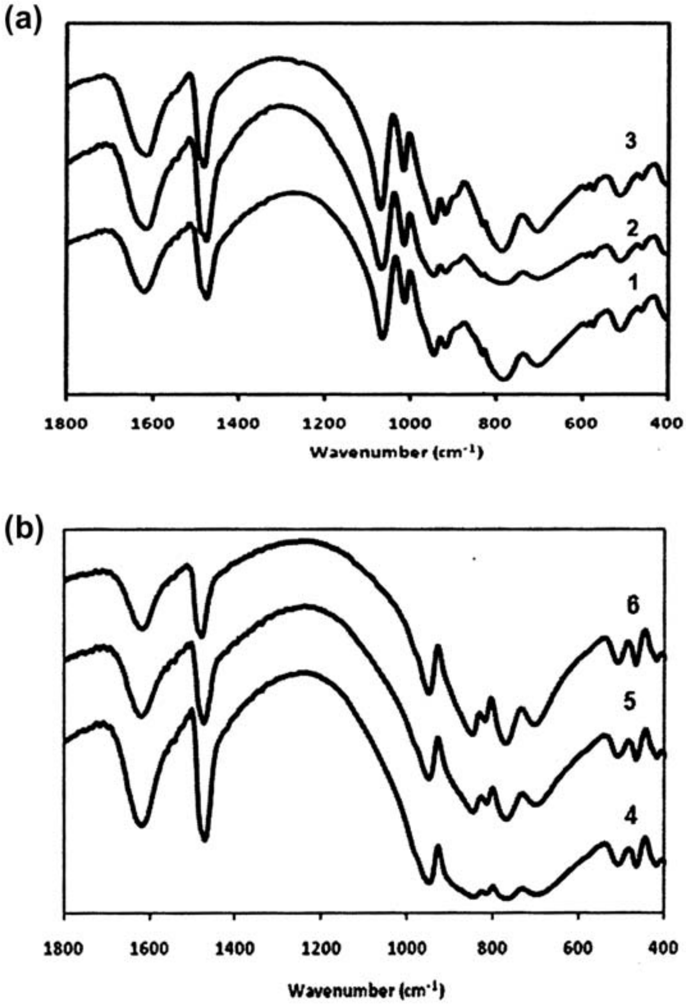

Figure 1. The IR spectra of (a) **1–3** and (b) **4–6** in KBr plate.

CO_2 at higher temperature than the arsenic-based complexes. The TGA curves are shown in Supplementary material.

3.4. *Electronic spectroscopy*

UV spectra of **1–6** exhibit two bands at -200 and -250 nm, assigned to $O_d \rightarrow W$ and $O_b/O_c \rightarrow W$ charge transfer transitions, respectively [41]. UV spectra of the complexes are similar, indicating similar electronic structures, shifted to higher wavelength on comparison with $[A\text{-}XW_9O_{34}]^{9-}$, due to coordination of lanthanide [27] (figure 2).

3.5. *Magnetic properties*

The values of $\chi_m T$ at 300 K for **1** and **4** are 34.67 and 35.43 $cm^3\ M^{-1}\ K$, close to the calculated value 35.46 $cm^3\ M^{-1}\ K$ for three non-interacting Tb^{3+} in the $^7F_6$, $(4f^8)$ ground

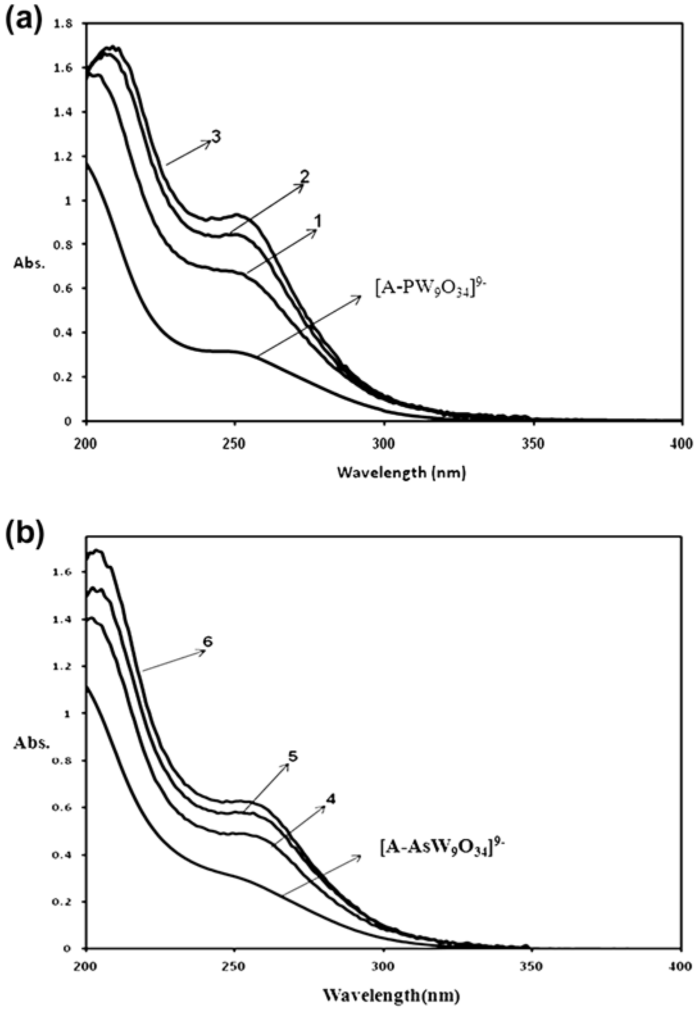

Figure 2. The UV spectra of 1×10^{-5} M of (a) **1–3** and (b) **4–6**.

state. The χ_mT values for **2** and **5** are 42.26 $cm^3\ M^{-1}\ K$, and 42.80 close to the calculated value of 42.54 $cm^3\ M^{-1}\ K$ expected for three Dy^{3+} ions in the $^6H_{15/2}$, ($4f^9$) ground state. The values of χ_mT for **3** and **6** are 33.64 and 33.78 $cm^3\ M^{-1}\ K$, lower than the calculated value 34.44 $cm^3\ M^{-1}\ K$ for three non-interacting Er^{3+} in the $^4I_{15/2}$, ($4f^{11}$) ground state [42, 43].

3.6. *Structures*

Ion–exchange experiments and UV spectra provide good evidence for bonding of the lanthanides to $[A\text{-}XW_9O_{34}]^{9-}$ in **1–6** [22, 28]. IR spectra, magnetic properties and TGA suggest that the complexes are isostructural with $[(A\text{-}PW_9O_{34})_2(H_2OY)_3CO_3]^{11-}$ [28] and $[(A\text{-}AsW_9O_{34})_2(H_2OM)_3CO_3]^{11-}$ ($M = Y^{3+}$, Sm^{3+}, Yb^{3+}) [37]. The ball-and-stick view of $[(A\text{-}AsW_9O_{34})_2(H_2ODy)_3CO_3]^{11-}$ (**5**) is shown in figure 3 together with the numbering

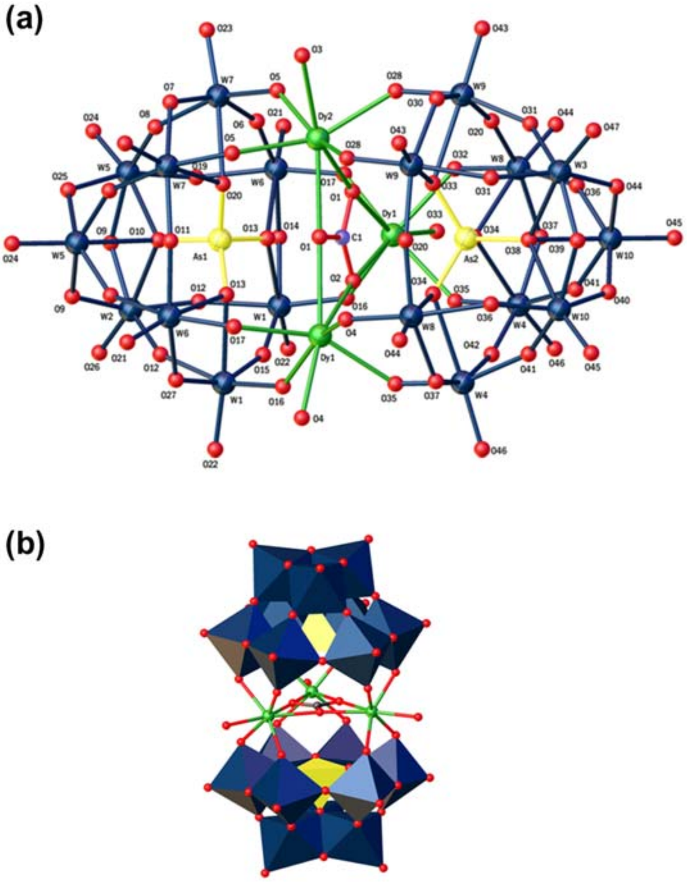

Figure 3. (a) Ball-and-stick representation of $[(A\text{-}AsW_9O_{34})_2(H_2ODy)_3CO_3]^{11-}$ (**5**); (b) Polyhedra representation of **5**.

schemes. The complex crystallizes in the orthorhombic Pnma space group, containing 10 W (W1–W10), 1As (As1), 2Dy (Dy1– Dy2), 44O, and 1C (C1) in the asymmetric unit. The structure of the complex consists of two lacunary $[A\text{-}AsW_9O_{34}]^{9-}$ Keggin moieties linked by a $(ODyOH_2)_3C$ belt into an assembly of virtual D_{3h} symmetry. The CO_3^{2-} is encapsulated in the Dy plane and ligated by its oxygens at the midpoints of the sides of the triangle formed by Dy^{3+} ions. Each Dy^{3+} adopts a mono-capped trigonal-prismatic coordination, the local 3-fold axis of DyO_6 lying in the regular triangular Dy_3CO_3 plane. The trigonal prismatic geometry is achieved by two terminal oxygens of an edge-shared pair of WO_6 octahedra to each $[A\text{-}AsW_9O_{34}]^{9-}$ and two oxygens from the belt. The cap is achieved by one external water [28, 37]. Two $[A\text{-}AsW_9O_{34}]^{9-}$ units in the complex are slightly distorted (As1–C1–As2 177.3°). As a result of this distortion the symmetry of the anion is reduced from D_{3h}. On the basis of valance bond sum (VBS) calculations, derived by Brown and Altermatt [44], oxygens of the belt are oxides (table 2). The Dy–O bond lengths in DyO_6 group and Dy–O(nW) are 2.260–2.463 Å, average 2.347 Å, and 2.375–2.410 Å, average 2.386 Å, respectively (table 2). VBS values for dysprosium, tungsten, arsenic and carbon are 2.84, 6.13, 5.05, and 4.06, respectively.

4. Conclusion

Six new complexes, $[(A\text{-}XW_9O_{34})_2(H_2OM)_3CO_3]^{11-}$ ($X = P^{5+}$, As^{5+}), ($M = Tb^{3+}$, Dy^{3+}, and Er^{3+}), were synthesized by the reaction of $[A\text{-}XW_9O_{34}]^{9-}$ with carbonate solution of M^{3+} and characterized by elemental analysis, IR and UV spectroscopies, TGA, and X-ray single-crystal structure analysis. The crystal structure of **5** consists of two lacunary $[A\text{-}XW_9O_{34}]^{9-}$ Keggin moieties linked by a $(OMOH_2)_3C$ belt to form A-type sandwich polyoxometalates.

References

[1] D.-L. Long, R. Tsunashima, L. Cronin. *Angew. Chem. Int. Ed.*, **49**, 1736 (2010).
[2] M.T. Pope, A. Müller (Eds.). *Polyoxometalate Chemistry: From Topology Via Self-Assembly to Applications*, Kluwer, Dordrecht, (2010).
[3] D.-L. Long, E. Burkholder, L. Cronin. *Chem. Soc. Rev.*, **36**, 105 (2007).
[4] B. Hasenknopf. *Front. Biosci.*, **10**, 275 (2005).
[5] I.V. Kozhevnikov. *Catalysts for Fine Chemical Synthesis*. Vol. 2. Catalysis by polyoxometalates, p. 216, Wiley & Sons, Chichester (2002).
[6] L. Xu, H. Zhang, E. Wang, D.G. Kurth, Z. Li. *J. Mater. Chem.*, **12**, 654 (2002).
[7] A. Muller, F. Peters, M.T. Pope, D. Gatteschi. *Chem. Rev.*, **98**, 239 (1998).
[8] E. Coronado, C.J. Gómez-García. *Chem. Rev.*, **98**, 273 (1998).
[9] T.J.R. Weakley, H.T. Evans, J.S. Showell, G.F. Tourné, C.M. Tourné. *J. Chem. Soc., Chem. Commun.*, 139 (1973).
[10] R.G. Finke, M.W. Droege, P.J. Domaille. *Inorg. Chem.*, **26**, 3886 (1987).
[11] J.M. Clemente-Juan, E. Coronado, J.R. Galan-Mascaros, C.J. Gomez-Garcia. *Inorg. Chem.*, **38**, 55 (1999).
[12] S.H. Wasfi, A.L. Rheingold, F.G. Kokoszka, A.S. Goldstein. *Inorg. Chem.*, **26**, 2934 (1987).
[13] X.Y. Zhang, Q. Chen, D.C. Duncan, R.J. Lachiotte, C.L. Hill. *Inorg. Chem.*, **36**, 4381 (1997).
[14] L.H. Bi, R.D. Huang, J. Peng, E.B. Wang, Y.H. Wang, C.W. Hu. *J. Chem. Soc., Dalton Trans.*, 121 (2001).
[15] N. Laronze, J. Marrot, G. Hervé. *Inorg. Chem.*, **42**, 5857 (2003).
[16] R. Khoshnavazi, L. Bahrami. *J. Coord. Chem.*, **62**, 2067 (2009).
[17] Y. Lu, Y. Xu, Y. Li, E. Wang, X. Xu, Y. Ma. *Inorg. Chem.*, **45**, 2055 (2006).
[18] R. Copping, L. Jonasson, A.J. Gaunt, D. Drennan, D. Collison, M. Helliwell, R.J. Pirttijarvi, C.J. Jones, A. Huguet, D.C. Apperley, N. Kaltsoyannis, I. May. *Inorg. Chem.*, **47**, 5787 (2008).
[19] L. Fan, L. Xu, G. Gao, F. Li, Z. Li, Y. Qiu. *Inorg. Chem. Commun.*, **9**, 1308 (2006).
[20] K. Binnemans. *Chem. Rev.*, **109**, 4283 (2009).
[21] H. An, Z. Han, T. Xu. *Inorg. Chem.*, **49**, 11403 (2010).
[22] M.A. AlDamen, S. Cardona-Serra, J.M. Clemente-Juan, E. Coronado, A. Gaita-Ariño, C. Marti´-Gastaldo, F. Luis, O. Montero. *Inorg. Chem.*, **48**, 3467 (2009).
[23] B.S. Bassil, M.H. Dickman, B. von der Kammer, U. Kortz. *Inorg. Chem.*, **46**, 2452 (2007).
[24] C. Boglio, G. Lemière, B. Hasenknopf, S. Thorimbert, E. Lacôte, M. Malacria. *Angew. Chem. Int. Ed.*, **45**, 3324 (2006).
[25] J.-P. Wang, X.-Y. Duan, X.-D. Du, J.-Y. Niu. *Cryst. Growth Des.*, **6**, 2266 (2006).
[26] W.H. Knoth, P.J. Domaille, R.L. Harlow. *Inorg. Chem.*, **25**, 1577 (1986).
[27] A.R. Tomsa, L. Muresan, A. Koutsodimou, P. Falaras, M. Rusu. *Polyhedron*, **22**, 2901 (2003); A.R. Tomsa, L. Muresan, A. Koutsodimou, P. Falaras, M.C. Bernard, V. Graban, M. Rusu. Synth. React. *Inorg. Met.-Org. Nano-Met. Chem.*, **36**, 335 (2006).
[28] X. Fang, T.M. Anderson, W.A. Neiwert, C.L. Hill. *Inorg. Chem.*, **42**, 8600 (2003).
[29] R. Khoshnavazi, S. Tayamon. *J. Coord. Chem.*, **63**, 3356 (2010).
[30] J. Hua, S. Li, X. Ma, P. Ma, J. Wang, J. Niu. *J. Coord. Chem.*, **65**, 1740 (2012).
[31] B. Chen, W. Chen, W. Liu, Y. Li, X. Wang, E. Wang. *J. Coord. Chem.*, **64**, 71 (2011).
[32] M.A. Aldamen, S.F. Haddad. *J. Coord. Chem.*, **64**, 4244 (2011).
[33] P.J. Domaille. *Inorg. Synth.*, **27**, 100 (1990).
[34] Bruker. *APEX2 Software Package*, Bruker AXS Inc., 5465, East Cheryl Parkway, Madison, WI 53711 (2005).
[35] G.M. Sheldrick. *Acta Crystallogr.*, **A64**, 112 (2008).
[36] A.J.C. Wilson (Ed.). *International Tables for X-ray Crystallography*, Vol. C, Tables 4.2.6.8 pp. 219–222 and 6.1.1.4 pp. 500–502, Kluwer Academic, Dordrecht (1992).
[37] R. Khoshnavazi, E. Naseri, S. Tayamon, A. Ghiasi-Moaser. *Polyhedron*, **30**, 381 (2011).
[38] K. Nakamoto (Ed.). *Infrared and Raman Spectra of Inorganic and Coordination Compounds*, Part B, 4th Edn, Planar XY_3 molecules pp. 121–125 and *Carbonate complexes*, Vol. 81, pp. 252–254, Wiley-Interscience, New York, NY (1986); R. Khoshnavazi, A. Salimi, A. Ghiasi-Moaser, *Polyhedron*, **27**, 1303 (2008).

[39] R. Khoshnavazi, S. Gholamyan. *J. Coord. Chem.*, **63**, 3365 (2010).
[40] R. Contant, R. Thouvenot. *Can. J. Chem.*, **69**, 1498 (1991); M. Rocchiccioli-Deltcheff, M. Fournier, R. Franck, R. Thouvenot. *Inorg. Chem.*, **22**, 207 (1983).
[41] M.T. Pope. *Heteropoly and Isopoly Oxometallates*, Springer-Verlag, New York, NY (1983).
[42] L. Liu, F. Li, L. Xu, X. Liu, G. Gao. *J. Solid State Chem.*, **183**, 350 (2010).
[43] C. Ritchie, M. Speldrich, R.W. Gable, L. Sorace, P. Kögerler, C. Boskovic. *Inorg. Chem.*, **50**, 7004 (2011).
[44] I.D. Brown, D. Altermatt. *Acta Crystallogr.*, **B41**, 244 (1985); H.H. Thorp. *Inorg. Chem.*, **31**, 1585 (1992); Available online at: http://www.ccp14.ac.uk/ccp/web-mirrors/i_d_brown/bond_valence_param/.